The Structure and Properties of African Wave Disturbances as Observed During Phase III of GATE[1,2]

RICHARD J. REED, DONALD C. NORQUIST[3] AND ERNEST E. RECKER

Department of Atmospheric Sciences, University of Washington, Seattle, 98195

(Manuscript received 7 September 1976, in revised form 15 November 1976)

ABSTRACT

A compositing method is used to determine the average structure and properties of eight wave disturbances observed over west Africa and the eastern Atlantic during the period 23 August–19 September, 1974, a period marked by well-developed and regular wave activity. The disturbance centers propagated westward in the zone of cyclonic shear to the south of the 700 mb easterly jet, located at 16–17°N. The mean wavelength was about 2500 km and the mean period 3.5 days. The mean zonal current satisfied the necessary condition for barotropic instability.

The composite disturbance was most intense at 650 mb, being cold core below and warm core above. Two circulation centers were evident at the surface, one located below the upper center and the other displaced 10° to the north at about the latitude of the monsoon trough. When separate composites were constructed for land and ocean stations, the dual centers were found to be primarily a land phenomenon. Distinctive features of the high-level (200 mb) circulation were a strong region of divergence located just ahead of the disturbance center and pronounced regions of anticyclonic and cyclonic vorticity situated several hundred kilometers to the north and south, respectively. Maximum low-level convergence and upward vertical motion were found in the region ahead and slightly south of the center. This was also the region of greatest convective cloud cover and largest precipitation amount.

Some minor differences are noted between wave behavior over land and sea. Over the ocean wavelengths were shorter, vorticities were greater at all levels, especially at the surface, and the horizontal wave axis was more tilted at levels close to the core of the mid-tropospheric jet stream. In association with the greater tilt, the northward momentum flux and transformation of zonal kinetic energy to eddy kinetic energy were stronger.

1. Introduction

A primary objective of the GARP Atlantic Tropical Experiment (GATE) is the study of the interaction of cumulus convection with features of the large-scale circulation. Central to the achievement of this objective is the identification of the synoptic-scale disturbances which traversed the GATE region during the period of the experiment and the determination of their structure and properties. The existence of westward traveling disturbances over west Africa and the eastern Atlantic during the months from June to October has long been known (e.g., Hubert, 1939). In particular, their importance as progenitors of some tropical storms and hurricanes in the western Atlantic has been remarked on by numerous authors (Piersig, 1936; Regula, 1936; Riehl, 1954; Erickson, 1963; Arnold, 1966; Simpson *et al.*, 1968; Frank, 1970). The African disturbances or waves have been studied extensively in recent years by Carlson (1969a, b) who used conventional synoptic and satellite data and by Burpee (1972, 1974) who used spectral and compositing techniques. Pedgley and Krishnamurti (1976) and Rennick (1976) have employed simple numerical models to investigate their origin and energetics.

The purpose of the present paper is to describe the structure and properties of the synoptic-scale disturbances which occurred over central and western Africa and the eastern Atlantic during Phase III of GATE and the preceding interphase period. During this interval from 23 August to 19 September, 1974, eight disturbances or waves, with average wavelength of nearly 2500 km and period of 3.5 days moved westward across the area of interest at a speed of 8 m s^{-1} (6–7° longitude day^{-1}). These waves were better organized and more uniform in behavior than those observed earlier in GATE and thus are particularly well-suited for compositing. The results which we shall describe are for the composite wave constructed from all surface and upper air data contained in the Quick Look Data Set[4]

[1] Research supported by the Global Atmospheric Research Program, Climate Dynamics Research Section, National Science Foundation, and the GATE Project Office, NOAA.

[2] Contribution No. 407 Department of Atmospheric Sciences, University of Washington.

[3] Present affiliation: Westinghouse Hanford, Richland, Wash. 99352.

[4] Prepared by Synoptic-Scale Subprogram Data Center (SSDC), Bracknell, England, and available on magnetic tape from World Data Center-A, Asheville, N. C.

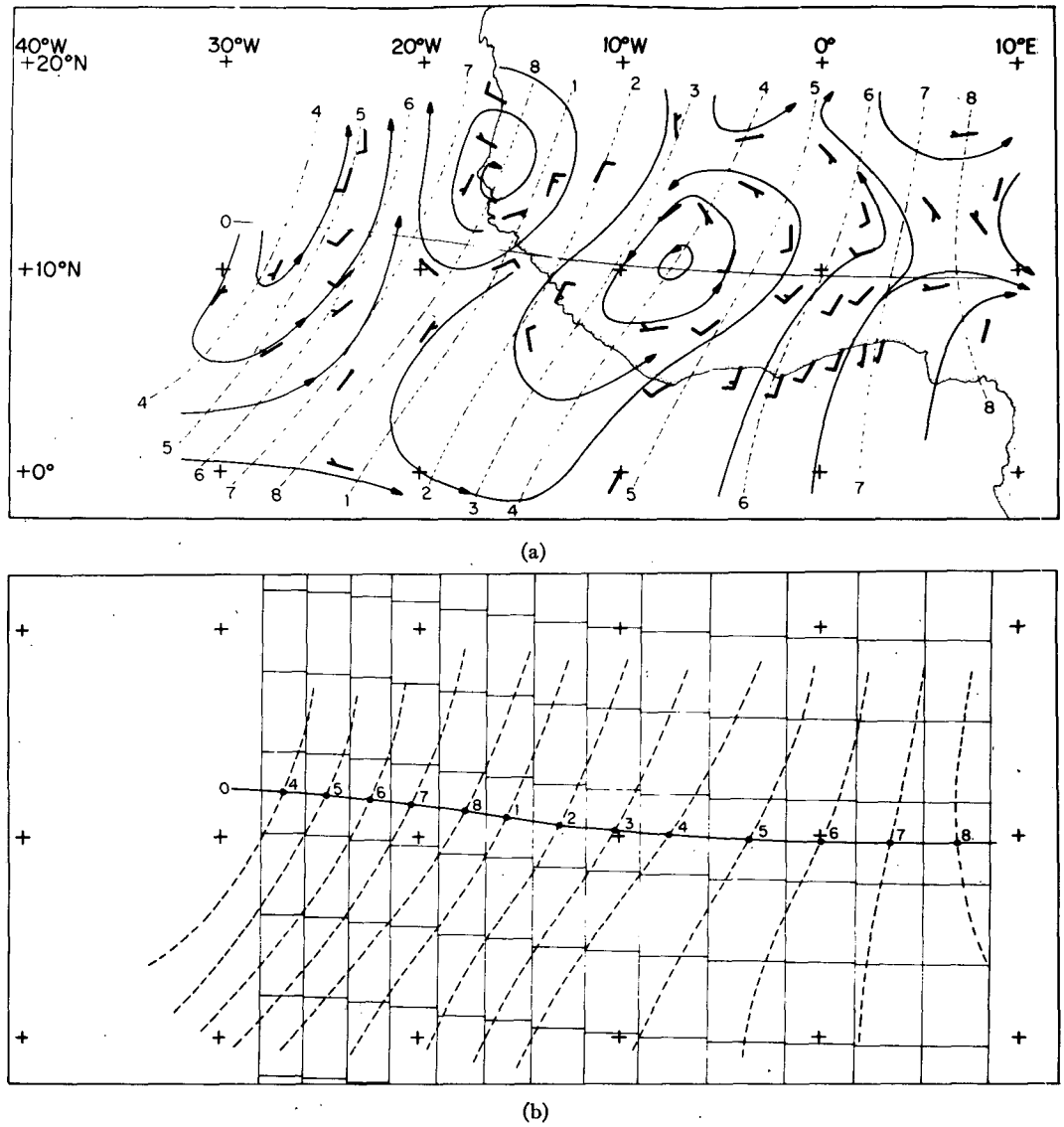

FIG. 1a. Streamline analysis with superimposed phase lines (dashed) and disturbance path (thin solid line) for 1200 GMT 7 September 1974. Band-pass filtered winds are plotted at station locations. Plotting convention: one full barb corresponds to 5 m s^{-1}, one-half barb to 2.5 m s^{-1} and no barb to 1m s^{-1}.

FIG. 1b. Boxes used in compositing.

for the period and area in question. Use was also made of subjectively digitized infrared brightness extracted at 6 h intervals from SMS 1 images for 1° latitude-longitude squares.

Burpee (1975) has previously published wave composites for the GATE period. The effort reported here differs in several respects from his earlier study: 1) It is restricted to Phase III when the waves were best developed. 2) A variable north-south coordinate is used in the compositing technique to sharpen wave structure. 3) Additional meteorological variables are treated. 4) A comprehensive attempt is made to relate convective activity and precipitation to the typical wave.

Our original purposes in undertaking the present study were to gain familiarity with the GATE data formats and reporting network, to develop computer programs for analysis of the data, and hopefully to obtain some preliminary results of interest while waiting for the final, validated data set to become available. It was, and still is, our intent to repeat the analysis using the final data set. Consequently, the decision was made to use the Quick Look Data Set in the form provided despite the realization that it contains many erroneous reports that could be weeded out with further editing. We have preferred, for the time being, to rely on the large size of the data sample to keep the errors within tolerable limits. The results suggest that this strategy has proved successful by and large.

2. Method

The compositing was accomplished by dividing each wave at each synoptic hour into 56 rectangular areas

TABLE 1. Number of observations of wind and satellite IR brightness and reported number of hours of precipitation measurement in various latitude belts. Upper left, land; upper right, ocean; center, total.

Latitude band	Wind				SMS-1 IR brightness	Precipitation measurement (h)
	Surface	700 mb	500 mb	200 mb		
6° to 10°	575/482	109/79	33/46	22/31	4657/1341	5736/2031
	1057	188	79	53	5998	7767
2° to 6°	1830/926	446/214	156/162	116/145	7662/3606	17 340/5676
	2756	660	318	261	11 268	23 016
−2° to 2°	2062/926	317/376	121/344	78/333	7728/3606	18 198/4125
	3011	693	465	411	11 334	22 323
−6° to −2°	2152/748	263/436	143/430	116/395	7728/3606	18 672/2148
	2900	699	573	511	11 334	20 820
−10° to −6°	553/222	92/137	80/138	71/132	6573/3353	3648/612
	775	229	218	203	9926	4260
Totals	7172/3327	1227/1242	613/1120	403/1036	34 348/15 512	63 594/14 592
	10 499	2469	1733	1439	49 860	78 186

or boxes, representing different regions of the wave, and by assigning each observation in the Quick Look Data Set to the appropriate box according to the position of the observation relative to the wave. The 56 boxes are arranged in eight columns, oriented north-south, each containing seven boxes. The middle box in each column is centered on the locus or path of the disturbance center at 700 mb, defined as the point of maximum vorticity. The width of the boxes in the north-south direction is 4° latitude.

The columns correspond to eight different wave phases, numbered 1 to 8, as in the previous study of Reed and Recker (1971). Category 2 is centered on the region of maximum northerly wind component, category 4 on the trough, category 6 on the region of maximum southerly component and category 8 on the ridge. Categories 1, 3, 5 and 7 occupy intermediate positions. The boxes are positioned so that the middle box in the column determines the phase category. Thus other boxes in the same column may be in different sectors of the wave. This arrangement allows the composite wave to determine its own tilt in the horizontal plane. Similarly, the wave is free to determine its own vertical slope, since the categories are prescribed at one level only, i.e., 700 mb. The eight categories span an average wavelength of approximately 2500 km, yielding an average box width of about 3° longitude.

The wave phases required for compositing were obtained from band-pass filtered 700 mb winds derived every 6 h from time series constructed for a large number of stations. The filter utilizes 15-point and 5-point running means to reduce waves of periods shorter than 2 days and longer than 6 days to less than half-amplitude, while retaining almost fully waves of 3–4 day period. Missing data were interpolated from maps prepared at Dakar during the field period and received on microfilm from World Data Center-A. An example of a filtered wind field and the associated phase lines appears in Fig. 1a. The figure also shows the area included in the phase analysis and the stations employed. Only actual unfiltered data were used in the compositing, and these were taken from a slightly larger area than shown—from 10°E to 31°W and from 1°S to 26°N. Fig. 1b depicts the wave boxes corresponding to the example in the figure above.

After the observations were assigned to the appropriate boxes, averages were taken at all standard levels between the surface and 100 mb to determine the composite fields of the pertinent variables. The raw variables treated were wind, temperature, dew point, precipitation amount and convective cloud amount. Relative humidity was determined from the temperature and dew point and divergence and vorticity from the composited wind field. The kinematic method was used to measure vertical p-velocities.

Table 1 indicates the vast number of observations that were available for the five inner rows. Here and in later figures latitude is measured with respect to the disturbance path. The zero or reference latitude, as it will be referred to hereafter, lies at an average latitude of 11°N over land and 12°N over the ocean. Figures for land refer to observations taken between

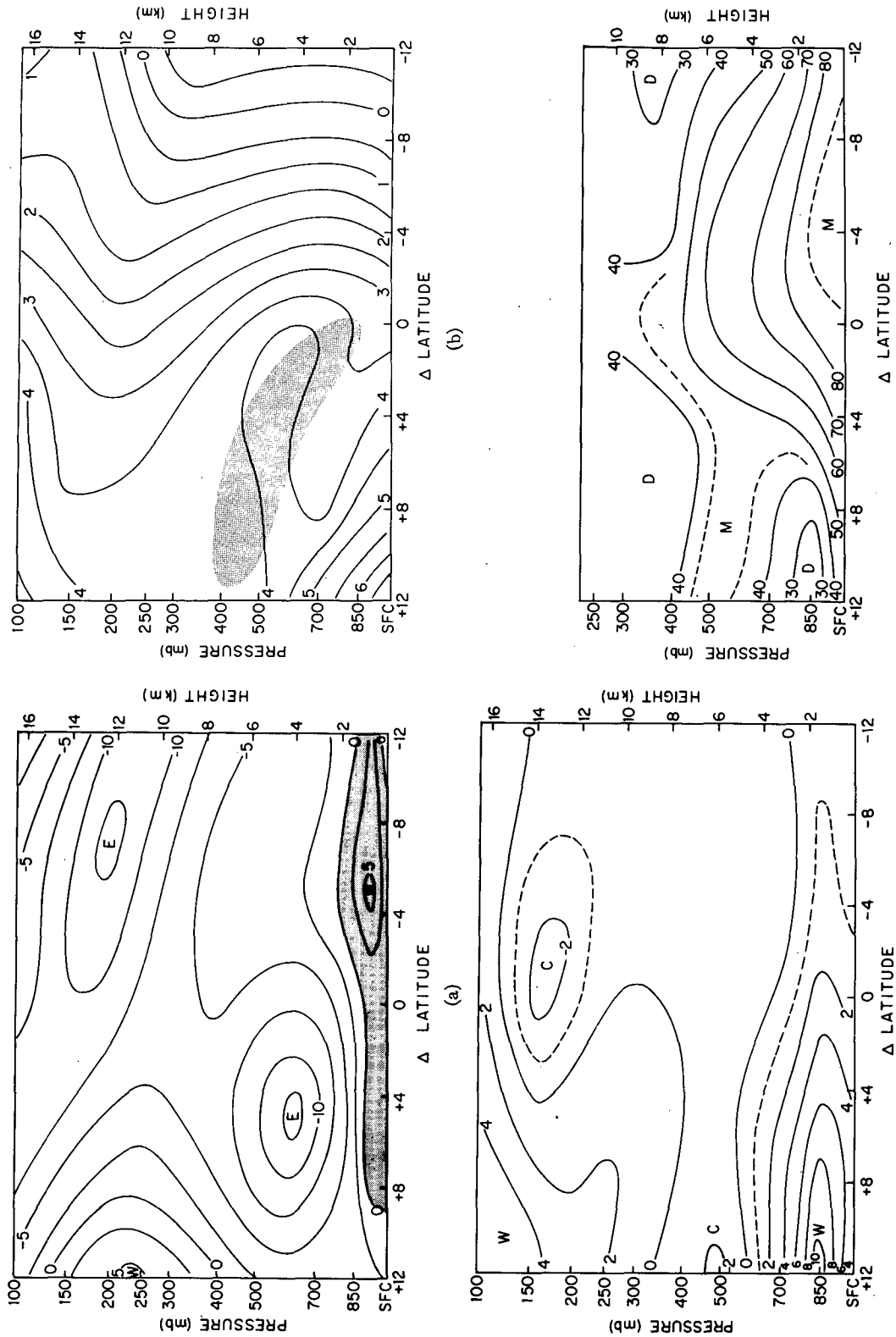

FIG. 2. Zonal mean fields (space and time) for period 23 August to 19 September, 1974. "Zero" latitude corresponds to average latitude of disturbance path, 11°N over land and 12°N over ocean. (a) Zonal wind ($m\ s^{-1}$); (b) absolute vorticity ($10^{-6}\ s^{-1}$); (c) temperature deviations (°C) from values at Δ latitude = −12; (d) relative humidity (percent).

10°E and 15°W, whether over land or sea, and for ocean refer to all observations between 15°W and 31°W including some coastal reports.

The number of radiosonde observations diminishes considerably with height. Even so, observations are plentiful in the innermost row where there are, for instance, an average of $411/8 \approx 51$ per box at 200 mb, a sufficient number to resolve well the wave features at that level. Adjacent rows also have ample numbers of observations. The amount of data is less adequate in the outer rows and in the outermost rows (not shown in the table) it is so limited that the analyses must be viewed with caution in the vicinity of the margins.

It will be noted that considerable differences exist in the amount of wind data available for land and ocean regions. At the surface roughly twice as many reports were received from land stations as from ocean. At the uppermost levels the opposite is the case. Similar differences exist for temperature and dew point except that the discrepancy is even larger aloft, the number of observations from ocean stations exceeding those from land by a factor of about 3. These differences must be kept in mind when interpreting the results which, unless otherwise stated, are based on data for both regions with each observation given equal weight. Clearly the overall results are biased in favor of one region or the other at levels where the data amount differs in the two regions and where real differences in meteorological conditions prevail.

3. Results

a. Mean fields

Before presenting and discussing the wave or perturbation fields, we will consider, for the sake of completeness, the mean fields on which the wave motions were superimposed. These will be presented in the form of meridional cross sections of zonal wind, absolute vorticity, temperature and humidity for the 28-day period of study. It will be helpful to keep in mind that the zero or reference latitude on the diagrams to be shown has a mean position of approximately 11°N.

The cross section of mean zonal wind component (Fig. 2a) shows the features that are known to characterize the flow over central and western Africa during the summer season (e.g., Carlson, 1969a): the shallow westerly monsoon current at low levels, the mid-tropospheric easterly jet stream, the upper tropospheric easterly jet stream and the extension of the mid-latitude westerlies at high levels. The low-level westerlies are strongest at the top of the frictional boundary layer 5° south of the reference latitude (~6°N), where they reach a mean speed of 5 m s^{-1} and where they have a maximum depth of 2 km. The core of the mid-tropospheric jet is located 5° north of the reference latitude (~16°N) at 650 mb. The peak speed is estimated to be 13 m s^{-1}. The upper tropospheric easterlies, possessing a similar maximum speed, are located 12° farther south.

The absolute vorticity (Fig. 2b) increases monotonically to the north over most of the cross section. However, there is a region in the vicinity of the mid-tropospheric easterly jet (shown by stippling) in which the gradient reverses. The reversal of the gradient is known to be a necessary condition for barotropic instability of the zonal flow (Kuo, 1949). Burpee (1971), using eight years of data, has previously demonstrated that the condition for barotropic instability is met at 700 mb in the vicinity of 5°E in summer. He has also shown (1972) that the mean potential vorticity gradient along an isentropic surface vanishes. From the work of Charney and Stern (1962) this is known to be a necessary condition for instability of an internal baroclinic jet.

The mean temperature field (Fig. 2c), expressed in terms of the departure of the temperature at a particular latitude from that at 12° south of the reference latitude (approximately the equator) exhibits two main features: 1) a strong temperature contrast in the lower troposphere between the warm Saharan air and the cooler air overlying the ocean waters to the south and 2) a relatively cool region in the upper troposphere just south of the reference latitude. This region will be shown later to lie in the zone of maximum convective activity. Thus it is conceivable that it is maintained by adiabatic cooling in the negatively buoyant upper portion of cumulonimbus clouds.

The field of mean relative humidity (Fig. 2d) shows an extensive region of high relative humidity in the lower troposphere near and south of the reference latitude. The moist air domes upward in the vicinity of the reference latitude and also has a northward extension in the middle troposphere. Since relative humidities at all levels were computed relative to water rather than ice, it is possible that the decrease in values above 500 mb at the more northerly latitudes is fictitious. The origin of the upper moist layer is not clear. Driest air is found over the Sahara at 850 mb where the relative humidity drops below 30%. The dryness is almost certainly produced by subsidence in the descending branch of the Hadley circulation.

b. Horizontal fields

In this section we present wind, vorticity, divergence, vertical motion, temperature and relative humidity fields at selected pressure levels. In some cases the total field—mean plus perturbed—is shown; in other cases the zonal mean for each latitude has been subtracted so that only the disturbed field is depicted. All fields have been smoothed longitudinally by harmonically analyzing the eight values in each row and retaining only the first two harmonics. The coordinates used in the diagram are wave category as the abscissa and latitude difference as the ordinate. The abscissa may be regarded as an approximately east-west axis along which a category width represents about 3° of longitude. A cross is entered on each diagram at coordinates

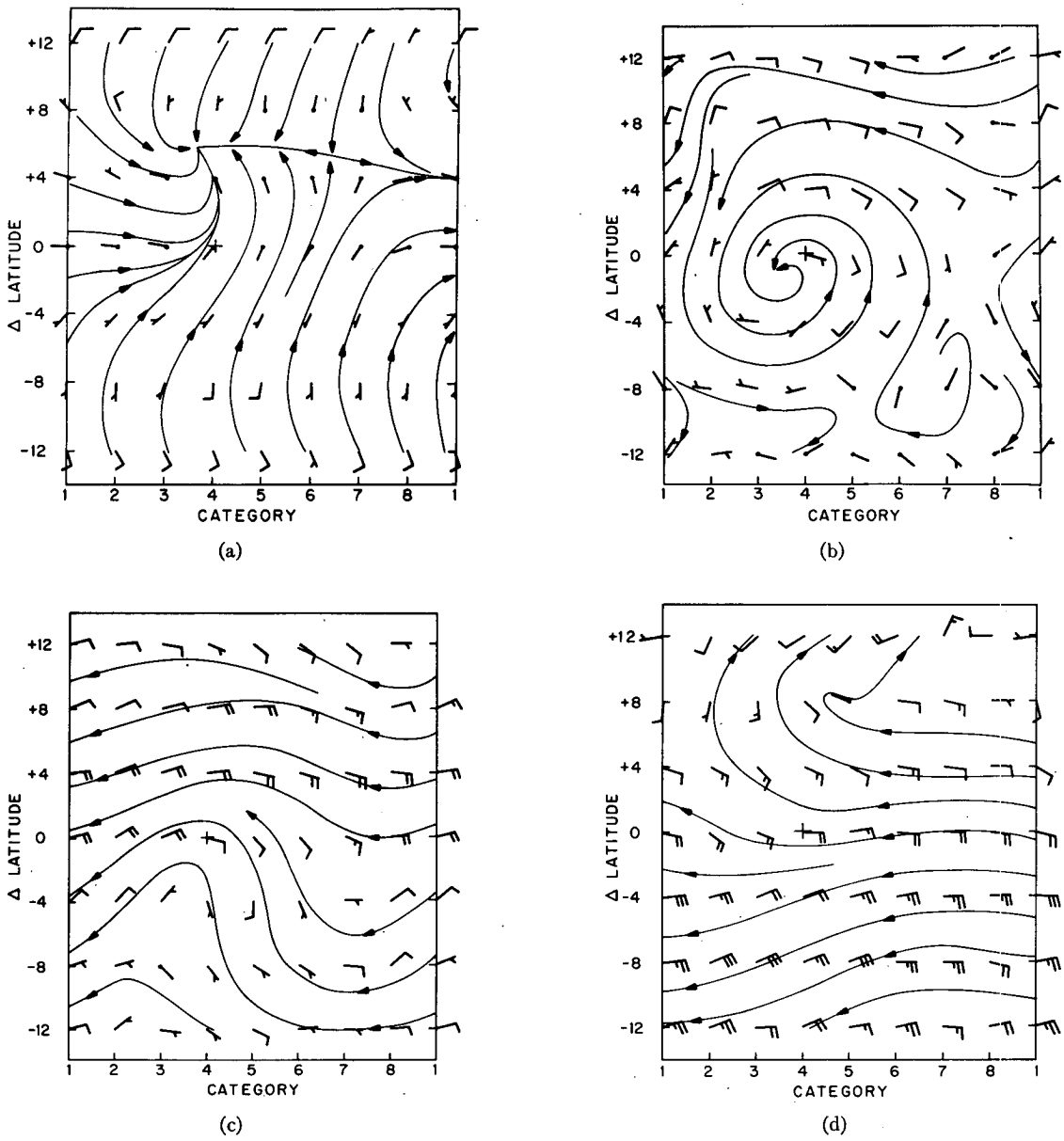

FIG. 3. Streamlines for the total wind field. Category separation is approximately 3° longitude. Cross denotes disturbance center at 700 mb. One full barb corresponds to 5 m s^{-1}, one-half barb to 2.5 m s^{-1} and no barb to 1 m s^{-1}. (a) Surface, (b) 850 mb, (c) 700 mb, (d) 200 mb.

(4,0). This denotes the position of the disturbance center at 700 mb, the chosen origin of the coordinate system.

The total wind fields at the surface, 850, 700 and 200 mb are displayed in Fig. 3. At the surface there exists a weak circulation centered about 5° north of the reference mark. Two main lines of confluence extend into the center from the east and south. At 850 mb the circulation is better developed, a closed center appearing just southwest of the reference mark. An open wave with pronounced northeast-southwest tilt to its axis is found at 700 mb. The tilt at the central and southern latitudes is similar to that observed by Burpee (1972, 1975) in previous studies. The easterly jet is seen at about 16°N (Δ latitude = +5). The extension of the disturbance into the upper troposphere is apparent in the substantial east-west variations that occur at 200 mb. A striking feature is the strong diffluence (and, as will be seen later, divergence) near and ahead of the reference mark.

The corresponding perturbation wind fields are shown in Fig. 4. The surface chart now shows the main center of cyclonic circulation to be located near the reference mark, about 6° south of its previous position. This result suggests the presence of two vorticity centers, one to the north where the mean flow has its greatest

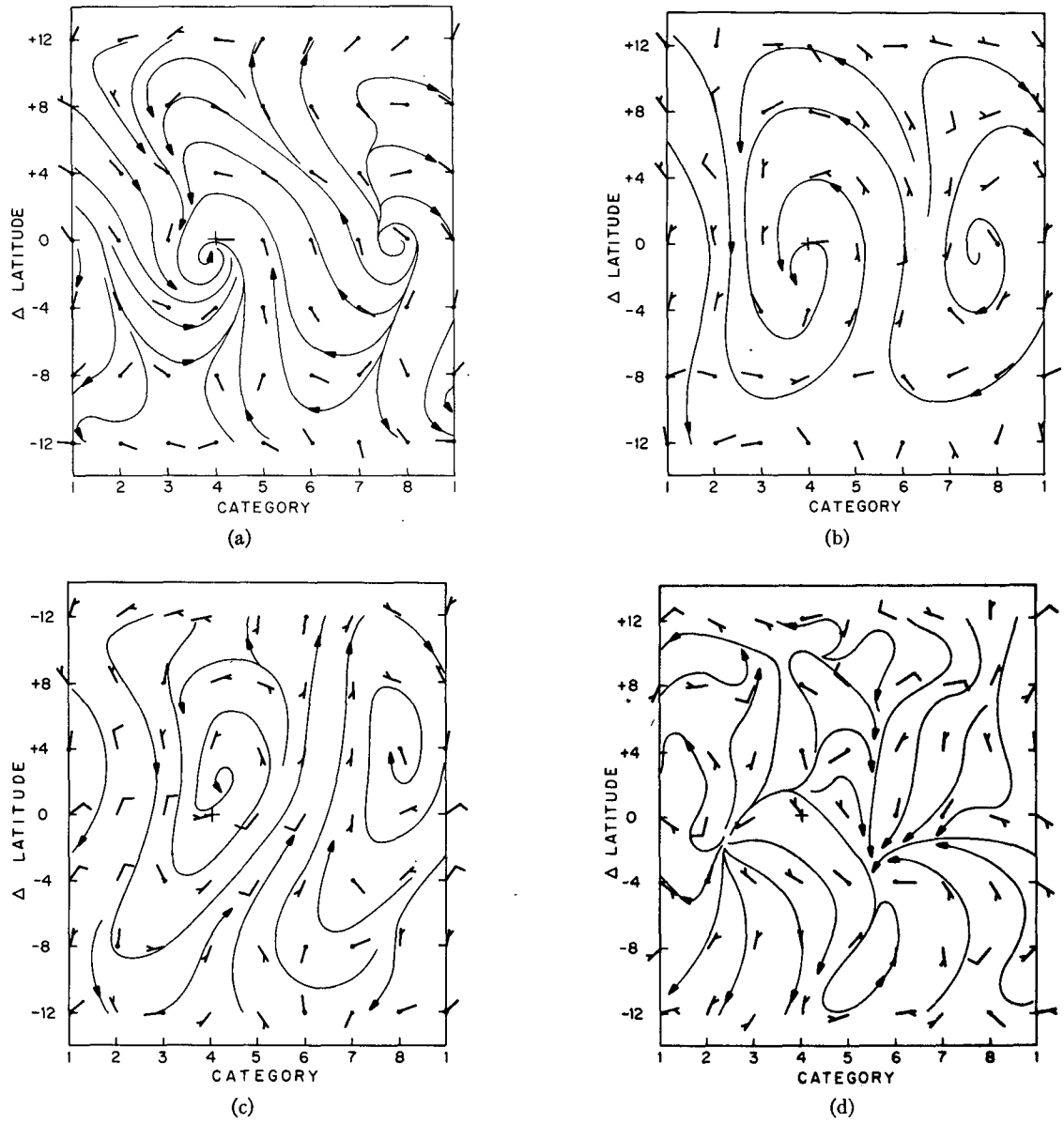

FIG. 4. Streamlines for perturbed wind field. (a) Surface, (b) 850 mb, (c) 700 mb, (d) 200 mb. See Fig. 3 for further description.

cyclonic shear and one to the south in the zone of active convection. Carlson (1969b) earlier remarked on the presence at the 2000 ft level of two cyclonic eddies in association with the upper wave. He noted that the more northerly one, located along the southern fringe of the Sahara, was relatively cloud-free, while the weaker one to the south was in a region of enhanced cloudiness. He proposed that the latter vortex was of convective origin. Burpee (1974) also called attention to the existence of two cyclonic circulations in the composite surface wind field obtained in his study.

Well-formed cyclonic and anticyclonic centers sloping northward with height are found at 850 and 700 mb. Very little east-west tilt of the wave axis is observed contrary to earlier results (Burpee, 1974, 1975). The 200 mb pattern is characterized by divergent and convergent flows near the reference latitude and pronounced cyclonic and anticyclonic flows displaced about 8° on either side. Burpee (1975) in his earlier study found little evidence of the waves at 200 mb along a cross section at 15°N depicting the meridional wind fluctuation. This finding is consistent with the lateral displacement of the rotational features noted above.

Vorticity fields at the surface, 850, 700 and 200 mb are shown in Fig. 5. The presence of a double maximum at the surface, as discussed previously, is evident in Fig. 5a. The stronger maximum lies to the north, near

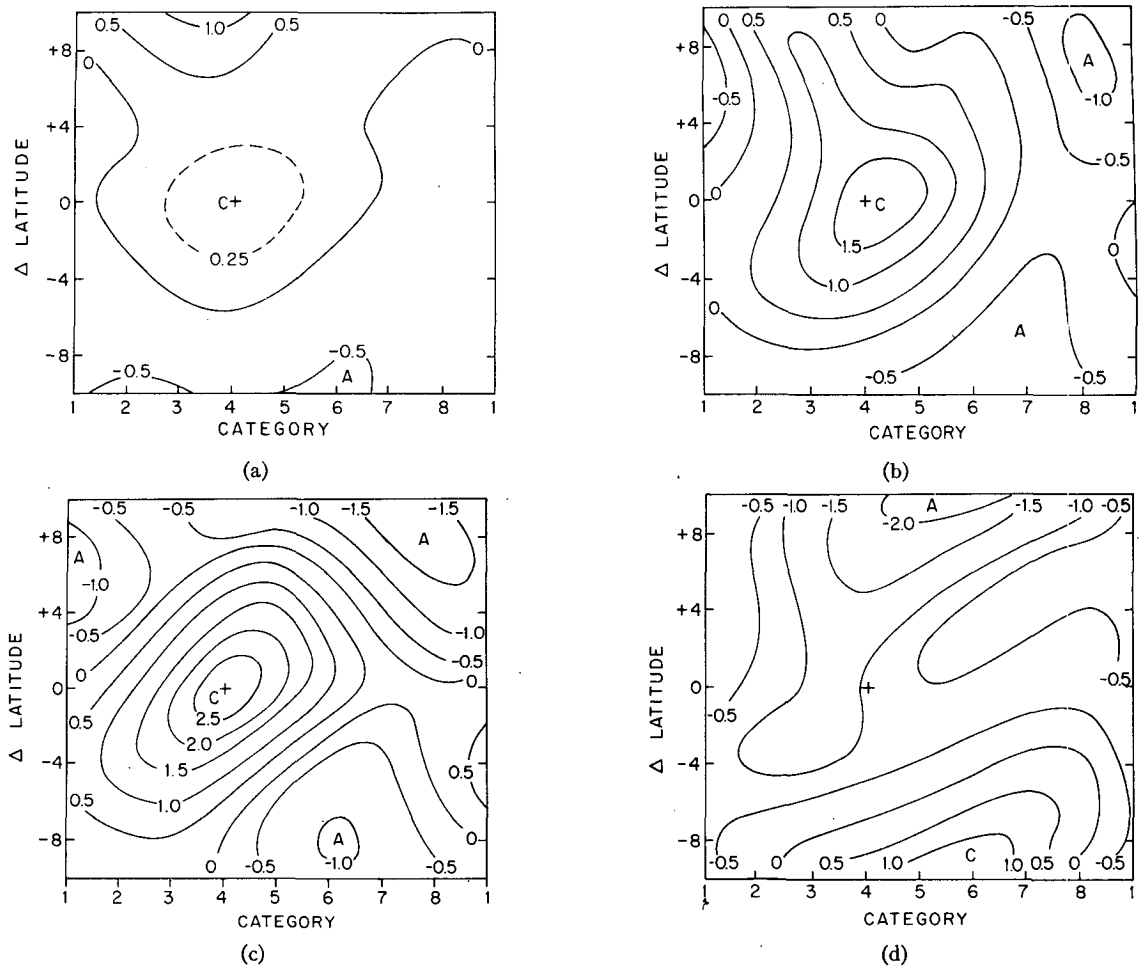

FIG. 5. Vorticity in units of 10^{-5} s^{-1}. (a) Surface, (b) 850 mb, (c) 700 mb, (d) 200 mb.

or over the Sahara. The second maximum is seen to represent a weak downward extension of the overlying upper level center. The strongest vorticity aloft occurs over the reference mark at 650 mb where it attains a value of about 3×10^{-5} s^{-1}. At 850 and 700 mb cyclonic vorticity tends to prevail along the reference latitude, the anticyclonic centers lying well to either side. The 200 mb chart exhibits anticyclonic vorticity along the northern border with the largest value in category 5. Along the southern boundary the vorticity is predominantly cyclonic with the region of largest value almost diametrically opposite the northern region of maximum anticyclonic vorticity. The fluctuations along the reference latitude are quite weak.

The divergence pattern (Fig. 6), expressed in terms of deviations from the zonal mean, shows convergence ahead of the wave trough at the surface and 850 mb and divergence behind. Largest magnitudes are at 900 mb (not shown). At 700 mb the pattern reverses, and at 200 mb intense areas of divergence and convergence are observed above the regions of low-level convergence and divergence, respectively. All divergences are mass balanced so that the pressure-averaged value in any vertical column is zero. From the few maps shown this fact may not be apparent.

The alteration of the raw divergences in order to achieve mass balance was accomplished by the method of O'Brien (1970) who showed that the correction at a given pressure level should be proportional to the error variance. Neglecting possible variations of measurement error with height, we have assumed in accordance with sampling theory that the error variance is inversely proportional to the number of wind observations at the level in question.

Vertical velocity deviations from the zonal means computed from the mass-balanced divergences are shown in Figs. 7a and 7b for the 850 and 300 mb levels. Strongest upward motions occur ahead of the wave axis in categories 2 and 3. The magnitude changes little between the two levels. The horizontal variations of the vertical velocity deviations are as large as 6 mb h^{-1} or 2 cm s^{-1}.

The perturbed temperature fields at 850 and 300 mb appear in Figs. 7c and 7d. In general the perturbations

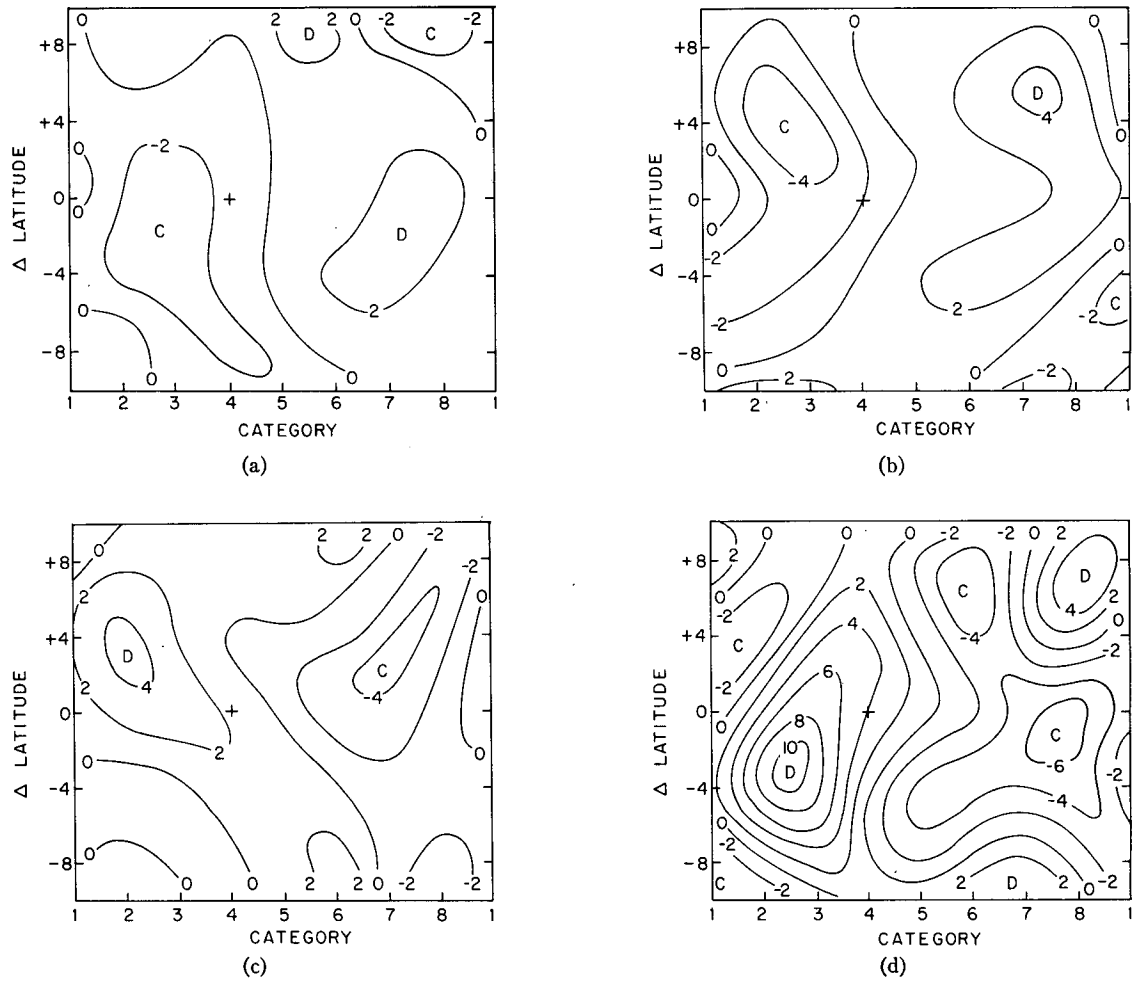

FIG. 6. Divergence deviation from zonal means in units of 10^{-6} s^{-1}. (a) Surface, (b) 850 mb, (c) 700 mb, (d) 200 mb.

are measured in fractions of a degree, a size typical of the tropical atmosphere. Coolest temperatures at low levels are found in the vicinity of the wave trough and warmest temperatures near the ridge. The regions of negative and positive anomalies slope westward with height, as will be seen in a later figure. Largest temperature anomalies, of about 1°C, occur at 850 mb in the region to the north of the reference latitude where the mean temperature gradient is largest (see Fig. 2c). The warm anomalies in that region tend to be correlated with northerly wind components and the cold anomalies with southerlies. The consequent southward directed heat flux in a region where the temperature decreases to the south indicates that the waves are acquiring eddy available potential energy from zonal potential energy. A comparison of Figs. 7a and 7c reveals that in that same region warm (cold) anomalies are correlated with rising (sinking) motion, signifying a conversion of eddy available potential energy to eddy kinetic energy.

The temperature pattern at 300 mb tends to be patchy and therefore is perhaps of somewhat questionable accuracy. Even so there is a rather close correlation between the temperature anomalies and the vertical velocity deviations (Fig. 7b) in the sense that eddy available potential energy is being converted to eddy kinetic energy. Because the mean temperature gradient is nearly zero at that level, the correlation of warm anomalies with upward motion cannot be explained by a dry baroclinic process. Conceivably latent heat release can account for the association, as has been found in observational studies for other parts of the tropics by Nitta (1970), Wallace (1971) and others and in a numerical modeling study by Manabe *et al.* (1970). Quantitative measurements of the wave energetics will be presented in a companion paper (Norquist *et al.*, 1977).

The relative humidity (Figs. 7e and 7f) undergoes substantial fluctuations with the wave passage. In the lower troposphere (Fig. 7e) the largest variations are found slightly to the north of the reference latitude, relatively dry air appearing ahead of the wave axis and relatively moist air to the rear. Burpee (1974) has already commented on this pattern of humidity change,

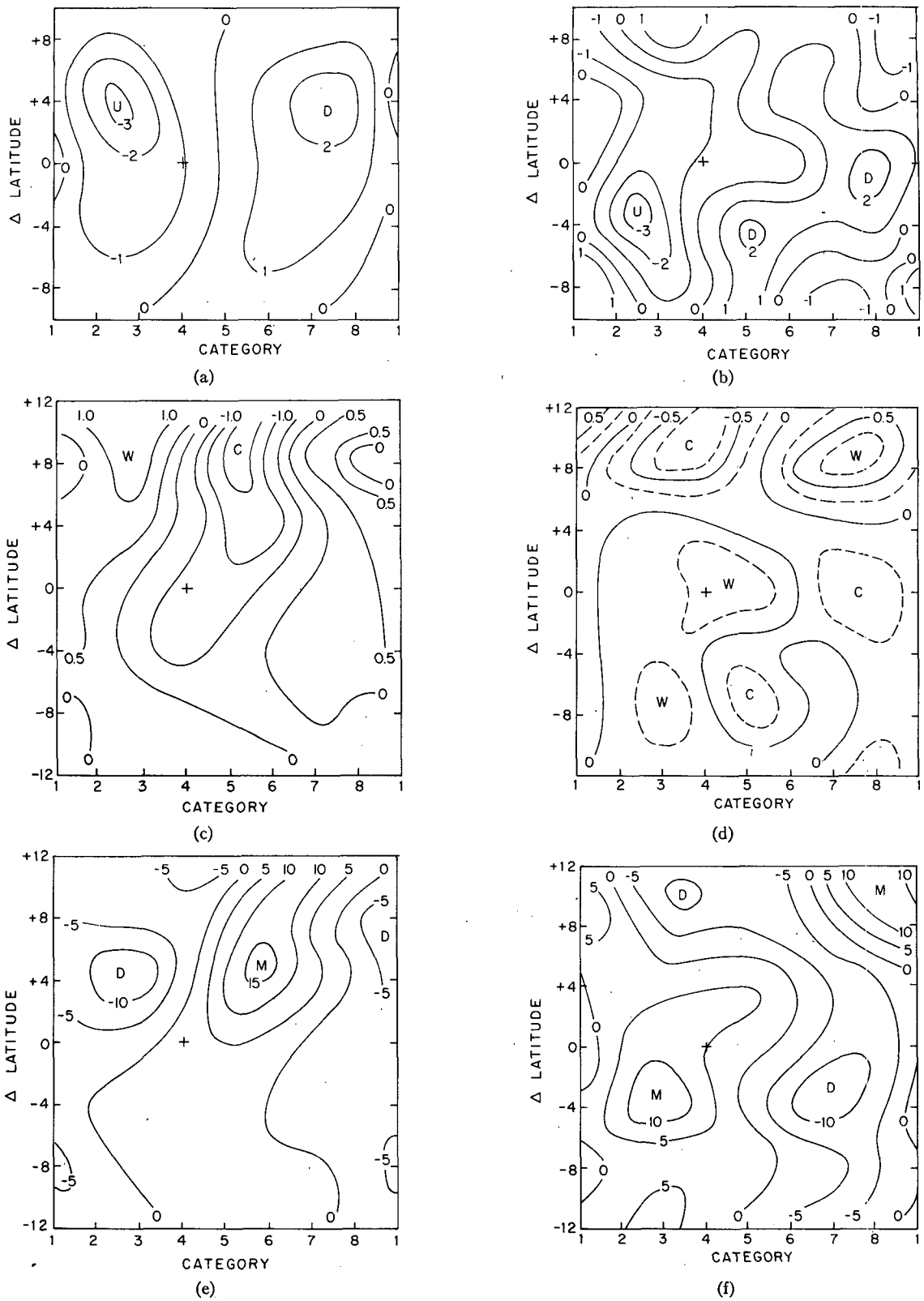

FIG. 7. Vertical motion deviation (mb h^{-1}) from zonal mean at (a) 850 mb, (b) 300 mb; temperature deviation (°C) at (c) 850 mb, (d) 300 mb; relative humidity deviation (percent) at (e) 850 mb, (f) 300 mb.

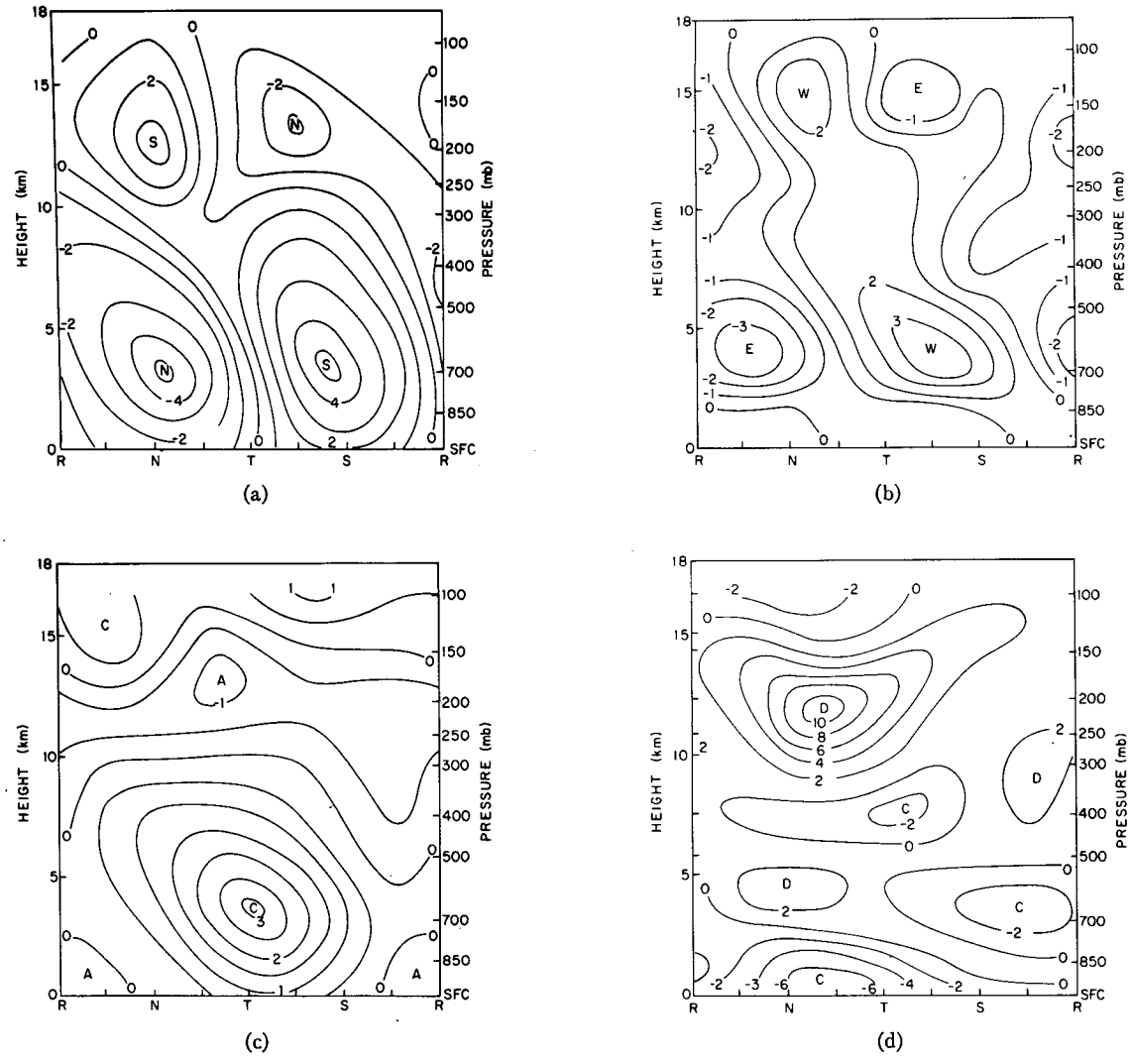

FIG. 8. Vertical cross sections along reference latitude. (a) Meridional wind deviation (m s^{-1}); (b) zonal wind deviation (m s^{-1}); (c) vorticity (10^{-5} s^{-1}); (d) divergence (10^{-6} s^{-1}). R, N, T, S refer to ridge, north wind, trough, south wind sectors of the wave, respectively.

attributing it to the southward transport of dry air from the Sahara in advance of the axis and the northward transport of moist monsoonal air to the rear of the axis, The largest anomalies of relative humidity at 300 mb (Fig. 7f) appear south of the reference latitude and are remarkably well-correlated with the vertical motion field shown in Fig. 7b. Vertical, rather than horizontal, moisture transport would seem to account for the pattern of anomalies at this level.

c. Vertical cross sections

The sections are taken along the reference latitude. In the cases of the divergence and vertical velocity, values for the three innermost rows have been averaged in order to obtain smoother results. Categories 2, 4, 6 and 8 are labeled N (northerly), T (trough), S (southerly) and R (ridge), respectively, on these diagrams.

The meridional wind component (Fig. 8a) has its largest fluctuation at 650 mb where the magnitude reaches 5 m s^{-1}. This is somewhat larger than reported in previous studies of Pacific and African waves based on compositing (Reed and Recker, 1971; Burpee, 1974, 1975). However, the difference can easily be accounted for by the variations of wave intensity that result from selecting different periods for study. Secondary maxima of opposite direction occur near 200 mb above the lower level maxima. It will be recalled that the fluctuations at high levels are noticeably stronger on either side of the plane of the cross section. The wave axis is nearly vertical below 700 mb and slopes westward above. Burpee (1974, 1975) found that in the vicinity of 15°N the axis slopes eastward with height below 700 mb and westward above. From Figs. 4a–4c, it is apparent that had the cross section been taken along

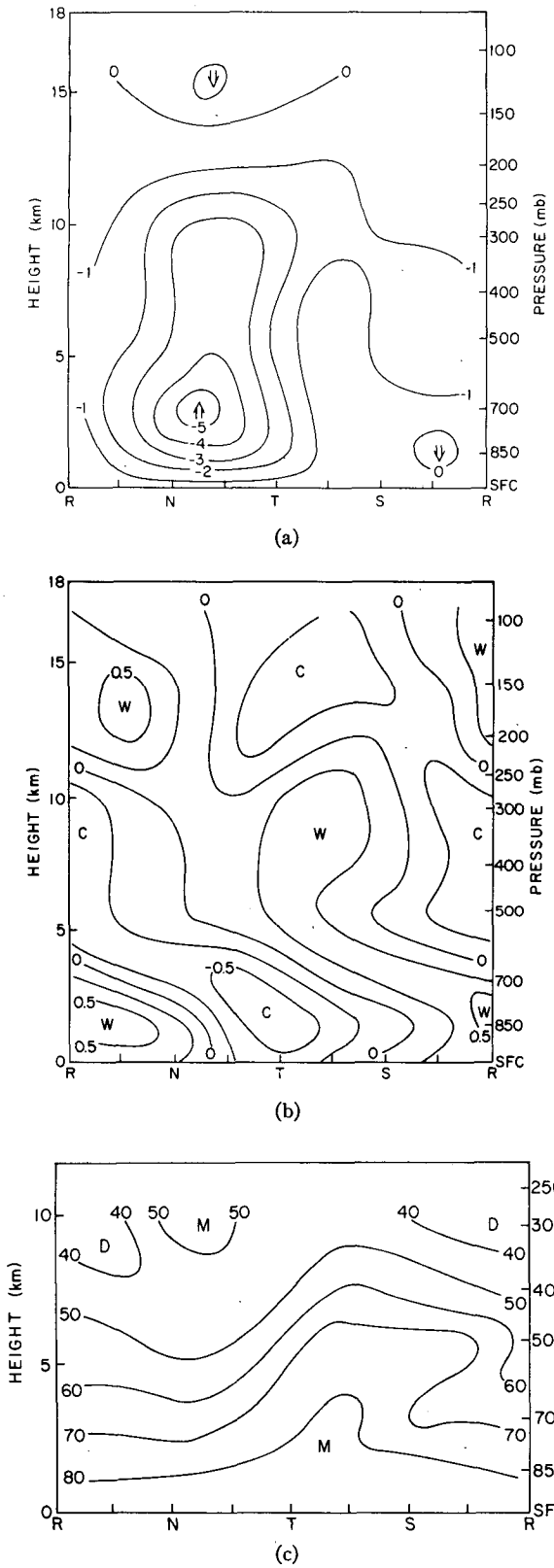

FIG. 9. As in Fig. 8 except for (a) vertical motion (mb h^{-1}), (b) temperature deviation (°C) and (c) relative humidity (percent).

15°N (Δ latitude=+4), a result similar to Burpee's would have been obtained. The opposite tilt of the wave axis at this latitude to the vertical shear of the zonal current is consistent with the previous deduction that baroclinicity contributes to wave growth in the sub-Saharan region. In the zone further south where the wave axis is vertical, the baroclinicity is weaker and precipitation is heavier so that latent heat release could play an important role in determining the temperature structure. Chang and Miller (1977) have shown that the axes of easterly waves in the Pacific tend to be more vertical during periods of anomalously warm sea surface temperatures. It seems probable that these are also periods of above normal precipitation or condensation heating.

According to Fig. 8b, the deviation of the zonal wind component from its latitudinal mean also exhibits substantial fluctuations. Regions of westerly and easterly wind anomalies correlate with regions of southerlies and northerlies, respectively, in the previous figure, an indication that the waves transport easterly momentum southward. The transport near 700 mb occurs in the region south of the easterly jet where the easterlies diminish with decreasing latitude. Thus the momentum transport is downgradient, and zonal kinetic energy is being transformed to eddy kinetic energy in agreement with earlier results of Burpee (1972). The magnitude of the transformation and its role in the maintenance of the wave disturbances will be treated in the aforementioned paper of Norquist *et al.* (1977).

The vorticity cross section (Fig. 8c) shows the previously mentioned maximum near 650 mb. Only a limited region of very weak anticyclonic vorticity appears at lower levels. More pronounced anticyclonic vorticity exists near 200 mb, the anticyclonic center aloft lying almost directly over the lower level cyclonic center. From Fig. 5d the upper minimum is seen to represent a southwestward extension of the main region of anticyclonic vorticity which appears along the northern fringe of the map.

The divergence pattern (Fig. 8d) is more complex than that found for Pacific systems (Reed and Recker, 1971). The strongest convergence, as noted previously, occurs close to the ground ahead of the trough. The maximum divergence lies above at the 200–250 mb levels. This height is lower than in the western Pacific and is consistent with the finding from radar and aircraft data that the height of the cumulonimbus anvils, and consequently of the region of mass outflow aloft was lower in the vicinity of the GATE B-scale ship network than had been expected from experience in other tropical areas (Burpee and Dugdale, 1975). Additional minor regions of convergence and divergence, whose significance is not understood, appear at intermediate levels. Possibly they are a consequence of the unique zonal wind profile that prevails in the west African region. Carlson (1969a) earlier speculated on

the existence of a convergence-divergence couplet at the level of the easterly jet.

The associated vertical motion pattern is shown in Fig. 9a. Strongest upward motion with a peak value of 5 mb h^{-1} (1–2 cm s^{-1}) occurs in advance of the wave trough. The magnitude is similar to that in the western Pacific composite of Reed and Recker but the peak occurs at a much lower level, 700 mb as opposed to 400 mb. A similar difference was noted during Phase II of GATE (Schubert and Reed, 1975). Subsidence is exceedingly weak in the vicinity of the reference latitude, being observed only in small regions near the 850 mb ridge and in the upper troposphere. The latter region may be fictitious. It should be mentioned that only the fluctuating part of the vertical motion field in Fig. 9a was obtained from the composite wind field. Because of the cyclic condition in the east-west direction, the composite field cannot be used to determine the zonal mean vertical motion. To measure the latter we have applied the kinematic method to geographically fixed triangles of wind observations, using all reports received from the principal wind reporting stations during the 28-day period.

The pattern of temperature anomalies (Fig. 9b) shows a cold core in the trough at levels below 700 mb and relative warmth above centered at 300–400 mb. This result, taken in conjunction with the previous finding of a vorticity maximum at 650 mb, indicates that the thermal wind relationship is being obeyed, at least qualitatively. Carlson (1969a) and Simpson *et al.* (1969) earlier reported a similar temperature structure. At still higher levels cold anomalies reappear.

The relative humidity (Fig. 9c), as noted previously, is highest where winds are southerly and lowest in the regions of northerly winds. In many respects the pattern resembles that found by Burpee (1974) for Dakar and by Reed and Recker (1971) for the western Pacific except that the driest air at low and middle levels tends to be more closely in phase with the northerly flow than in the Pacific study. At high levels a reversal occurs so that the moistest air lies above the region of relative dryness at low levels. As discussed already, this is the region of strongest upward motions. If, as the results of the next section suggest, the mass flux is largely accomplished by convective updrafts, it is indeed possible to maintain dryness at intermediate levels while moistening the layer above.

d. Relationship of convection and precipitation to the wave

Fields of convective cloud and precipitation amount are given in Fig. 10. The former field was obtained from infrared brightness estimated subjectively at 6 h intervals from SMS 1 imagery for each 1° latitude-longitude square in the region extending from the equator to 20°N and from 10°E to 30°W. One of three levels of brightness was assigned depending on whether the square appeared predominantly black, gray or white.

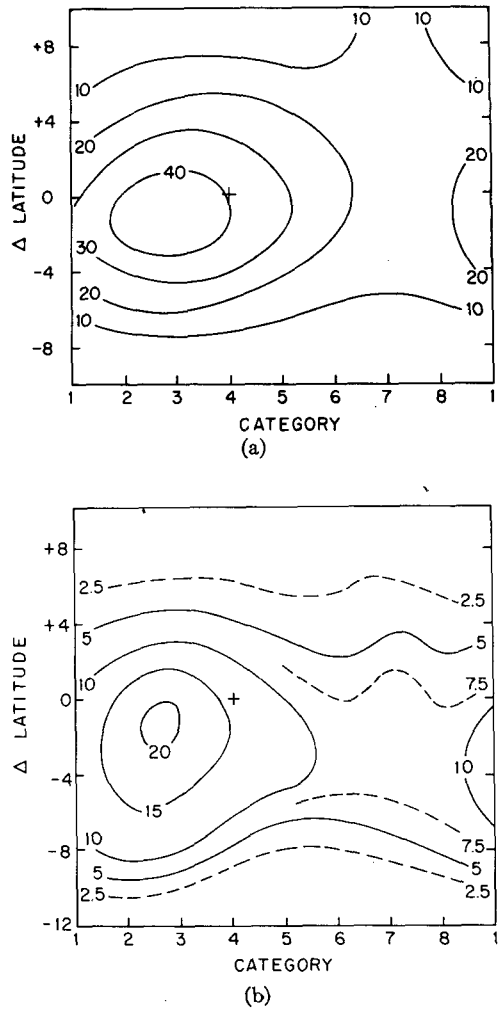

FIG. 10a. Percentage cover by convective cloud defined as white appearing cloud in SMS-1 infrared images.
FIG. 10b. Average precipitation rate (mm day^{-1}).

It is assumed that white appearing clouds are of convective origin.

The amounts in Fig. 10a are expressed in terms of the percentage of observations in a 3° square which were designated as white or convective. Thus they represent both time and space averages. From the figure it is evident that a nearly threefold modulation of the convection by the wave occurs in the vicinity of the reference latitude with the maximum activity taking place just ahead and slightly to the south of the disturbance center at 700 mb. The position more or less coincides with that of the strongest surface convergence (Fig. 6a). At higher latitudes the largest amount appears in category 7. At these latitudes, where the air is drier on the average, it may be that the convective activity is particularly sensitive to the low-level moisture supply, as Burpee (1974) has suggested. From Fig. 7e it is seen that the positive anomaly of relative humidity is indeed displaced eastward in the northerly

region, though not sufficiently to constitute an entirely satisfactory explanation. Alternatively, it may be that the cloud in question is not connected with ground-based convection but forms at middle levels (Simpson and Simpson, 1975) as a consequence of some subtle feature of the large-scale motion field. We say this because the same feature appears over the cooler ocean waters when the compositing is carried out for an oceanic subregion.

The distribution of precipitation with respect to the wave, expressed in millimeters per day, is presented in Fig. 10b. On the whole it resembles the distribution of convective clouds, though some small differences are apparent, most notably the somewhat further westward position of the rainfall maximum and the greater extension of large amounts to the south. The latter feature might be assumed to be caused, at least in part, by the heavy rain that falls from relatively shallow clouds along the African coast south of 10°N. However, a close inspection of the data reveals that the same feature prevails over the GATE ship network and that there the daily rates are excessive in terms of the observed total rainfall for the period (Seguin *et al.*, 1976). In fact the average rainfall rates at all latitudes in the figure are found to be excessive when compared to the amounts reported in *Monthly Climatic Data for the World*.[5]

The reason for the excessive rates is not known. A possible explanation is the incompleteness of the precipitation record in the Quick Look Data Set. The rates shown on the figure represent averages for all instances, whatever their duration, in which a precipitation amount, including zero, was reported. If there were a systematic tendency for reports not to be transmitted in cases of no rain, an inflation of the figures would result. In any event, the relative amounts are felt to be reliable in view of the general similarity of the pattern with the convective cloud pattern. We prefer to wait for the final data set before trying to resolve the conflict between average rates and accumulated amounts.

Previous studies (Carlson, 1969a, b; Burpee, 1972, 1974) have given varied and conflicting relationships between disturbed weather or precipitation and circulation features. We attribute the better relationships found in this study to the large quantities of brightness and precipitation data that were used and to the well-developed wave activity that prevailed during the period of study.

4. Land-ocean differences

From the description of Carlson (1969a) and others it is known that easterly wave disturbances commonly intensify as they approach the coast and then weaken, at least temporarily, during their passage over the eastern and central Atlantic. It is thus of some interest to try to discern differences in wave structure and behavior across the region of study. We have therefore divided the data sample into two parts, as indicated in Table 1, one part designated land, which includes reports from the region between 10°E to 15°W, and a second part termed ocean, comprised of data from the region between 15°W and 30°W. We have then constructed composite maps of all quantities for the individual regions.

Burpee (1975) in his study of the GATE data made a similar division and concluded that the regional differences were too small to justify presenting separate results. Generally our results lead to the same conclusion. In most cases the observed differences are small enough to be attributed to sampling fluctuations. However, in some instances they appear to be real, either because of their size or because of supporting physical arguments. We now will consider cases in which the differences are judged to be significant.

1) The basic wave parameters themselves display a substantial difference in the two regions. The wavelength and period are longer over land than over the ocean—2700 km compared with 2200 km and 3.7 days compared with 3.2 days. The wave speed remains nearly the same. A similar shortening of the wavelength as the disturbances pass from land to sea was noted by Arnold (1966). Fig. 1a provides an example of the described wavelength difference and also shows another commonly observed feature—greater tilt of the phase lines over the ocean region. Since the basic fields differ little from 700 mb upward from one region to the other, the different behavior must somehow be connected with low-level changes in the wind and thermal structure. The disturbances generally have a northward component of motion in traveling from the interior to the coastal zone and adjacent waters. Fig. 1a again provides an example of such behavior which from examination of the mean 700 mb chart (not shown) seems readily explainable in terms of steering by the middle-level flow.

2) In association with the well-known southward displacement of the monsoon trough over the ocean, there is a corresponding southward displacement of the surface circulation center in the *total* wind field (not shown). The position of the center in Fig. 1a is a compromise between the land and ocean extremes. However, for both land and ocean regions the center of the *perturbed* circulation is located close to that for the combined regions (see Fig. 2a). It seems clear, as earlier suggested by Carlson (1969b), that two vortex centers exist over land, one in the monsoon trough near 20°N and a second near the 700 mb disturbance center at about 10°N. The two tend to merge over the ocean because of the southward dip of the monsoon trough.

[5] Sponsored by the World Meteorological Organization in cooperation with the U. S. National Oceanic and Atmospheric Administration. Available from National Climatic Center, Federal Building, Asheville, N. C. 28801.

3) The 700 mb perturbed flow is stronger over the ocean than over the land and the tilt of the wave axis is greater over the ocean. Thus the northward momentum flux is stronger by a significant factor. The barotropic energy conversion is correspondingly greater, as measurements to be presented elsewhere will show (Norquist *et al.*, 1977). The explanation for this behavior is not apparent.

4) The cyclonic vorticity in the disturbance is stronger over the ocean than over land. This is illustrated in Table 2, which gives average values at the surface and 850 mb for the reference mark and the eight surrounding points. Since, as stated previously, the disturbances are generally observed to strengthen as they approach and cross the coast, this result is not unexpected. The effect is bigger at the surface, suggesting that the difference in surface friction between land and sea also plays a part in producing the vorticity difference. If friction is a factor, one might also anticipate that the surface vorticity undergoes a daily variation over land in association with the diurnal heating cycle. Largest values should be observed during the warmest part of the day when the downward mixing of vorticity is strongest. To test this hypothesis we have further divided the data in Table 2 according to synoptic hour. It is apparent that a large difference in the correct sense exists at the surface. At 850 mb, on the contrary, the vorticity is essentially the same at both hours.

Over the ocean the vorticity also changes between 0000 and 1200 GMT despite the much reduced size of the heating cycle. Since coastal reports were included in the ocean data set, it is possible that the result is not fully representative of oceanic conditions. However, in view of the preliminary finding of a daytime maximum of convective activity and precipitation over the ocean (Martin, 1975; Marks, 1975), the effect could well be real. Moist convection can act to increase the vorticity near the surface in two ways: first by the mixing mechanism described above and second by the effect of the associated low-level convergence. Thus, it appears that vertical mixing and large-scale convergence associated with convection must be taken into account in fully explaining the variations in vorticity.

Burpee (1974) has presented power spectra of the surface meridional wind component which also indicate stronger wave development during the day over land.

TABLE 2. Average vorticities (10^{-6} s^{-1}) in the vicinity of the disturbance center.

	Surface		850 mb	
	Land	Ocean	Land	Ocean
0000 GMT	0.2	2.7	9.9	13.1
1200 GMT	2.1	5.6	10.0	15.3
Average	1.2	4.2	10.0	14.2

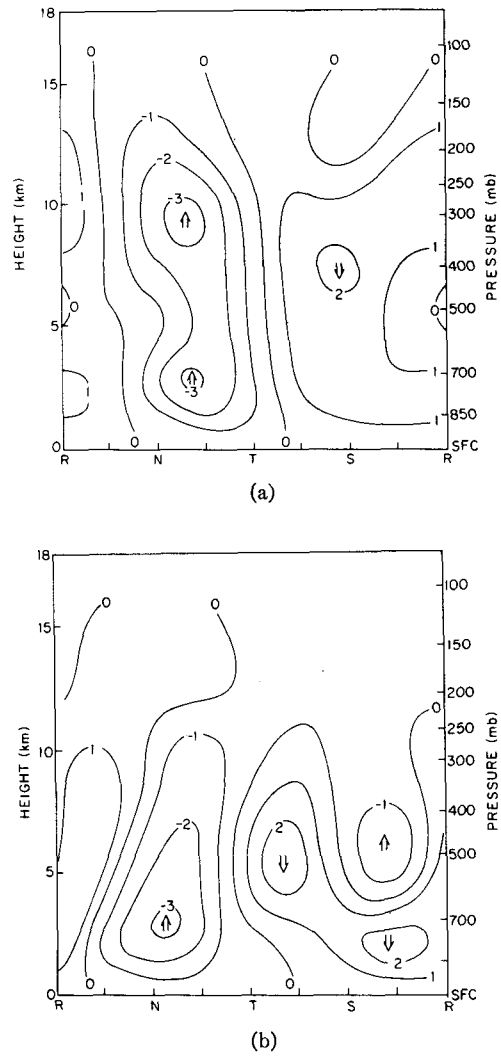

FIG. 11. Vertical motion deviation (mb h^{-1}) from zonal means for (a) land region (b) ocean region.

He did not present corresponding results for upper levels; however, it seems clear from the foregoing results that the large diurnal effect is confined to the near surface levels.

5) Finally there appears to be a significant difference in the pattern of vertical motion over land and sea. This is illustrated in Fig. 11 which shows the deviations from the zonal means for the two regions. Over land larger upward motions are found at the higher levels, suggesting the presence of deeper convection in that region. As mentioned previously, the convection over the GATE ship array was not as deep on the average as in many other regions of the tropics. A second difference is noted just ahead of the ridge where a region of upward motion appears at 500 mb over the ocean. A similar, but much weaker feature, displaced somewhat to the east, is found over land.

5. Conclusions

The main conclusions of the present study are as follows:

1) During Phase III and the previous interphase period, eight wave disturbances moved westward across the GATE area at an average speed of 8 m s^{-1}. Their wavelengths averaged about 2500 km and their periods about 3.5 days. They were centered in the cyclonic shear zone south of the easterly mid-tropospheric jet. The necessary condition for barotropic instability was met in the region of the jet.

2) The wave axis had a pronounced northeast-southwest tilt in the vicinity of 700 mb in conjunction with which there was a strong northward transport of westerly momentum and a conversion of zonal kinetic energy into eddy kinetic energy.

3) In the vicinity of the disturbance path (near 10°N) the systems, as judged from the perturbed wind field, were essentially vertical below 700 mb and sloped westward above. In the region of strongest baroclinicity to the north of the path they sloped eastward with height in the easterly shear zone below 700 mb suggesting that baroclinic wave growth occurs in this region. The wind perturbations were strongest at 650 mb and weakened with height, almost disappearing near 300 mb. A second maximum in the perturbed wind occurred in the vicinity of 200 mb. From the total wind field it appeared that the surface center was displaced sharply to the north of the center aloft. However, it is believed that the northern center is a separate phenomenon generated by interaction of the wave with the vorticity field of the monsoon trough.

4) The disturbances were cold core below 650 mb, warm core between that level and 250 mb and cold core at still higher levels. Consistent with the thermal wind equation, the vorticity was largest (3×10^{-5} s^{-1}) at the 650 mb level. The largest anticyclonic vorticity was observed in the upper troposphere centered well to the north of the lower level cyclonic center.

5) Largest temperature fluctuations occurred at 850 mb in the region of strong temperature contrast north of the disturbance track. Warmest temperatures and largest humidity deficits were associated with northerly winds, as would be inferred from the presence of the Sahara to the north. The negative correlation between the temperature and the meridional wind component indicated a conversion of zonal available potential energy to eddy in that region.

6) Strongest convergences (-7×10^{-6} s^{-1}) were measured near the surface somewhat ahead and south of the 700 mb disturbance center. The overlying divergence (10×10^{-6} s^{-1}) was strongest near 200 mb. The divergence pattern, however, was more complex than found elsewhere in the tropics, showing additional centers at intermediate levels.

7) The strongest upward motion (5 mb h^{-1}) was found at 700 mb in advance of the trough. Along the disturbance path subsidence was almost absent, being confined to a small region near the ridge. Upward motion was correlated with warm temperature anomalies in the baroclinic zone around 850 mb and rather generally in the layer about 300 mb, suggesting the possibility that the waves were maintained, at least in part, by a baroclinic energy conversion. However, there were levels and regions in which upward motion was associated with cold anomalies, making it impossible to estimate the sign of the net conversion by inspection.

8) A definite relationship was found between the wave pattern and the convective cloud and precipitation amounts. Both amounts were largest in the region where the strongest upward motions were measured and both showed nearly a threefold modulation with passage of the wave.

9) In general the wave characteristics were nearly the same over land and water. Some differences were observed, however, which are believed to be real. The wavelength and period were shorter over the ocean. Also the waves were somewhat stronger and their axes more inclined over the ocean so that the northward momentum flux and associated barotropic energy conversion were greater. At the surface twin vorticity centers, separated by about 10° latitude, were observed over land. Over the ocean they appeared to merge into a single center. Surface vorticities exhibited a large day-night difference especially over land. This is believed to be connected with diurnal variations in the boundary layer frictional stress and the convective activity. The rising motions in the wave were weaker in the upper troposphere over the ocean suggesting that the convection was not as deep there on the average as over land.

This paper has dealt mainly with the structure and properties of the wave disturbances. A question of fundamental importance, concerning which some brief comments have been made, is the processes responsible for the generation and maintenance of the waves. From the fields presented it is possible to make quantitative measurements of the various forms of energy and of the conversions from one form to the other. The results of such measurements will be reported in a companion paper (Norquist *et al.*, 1977). The composited data are also suitable for determining heat, moisture and vorticity budgets and for diagnosing properties of cloud ensembles. Work is progressing on these aspects of the wave description.

Acknowledgment. We are grateful to Mary McGarry and Steven Payne for providing the subjectively digitized SMS 1 infrared brightness data. We would also like to thank Professors J. R. Holton, H. Tennekes and J. M. Wallace for helpful discussions.

REFERENCES

Arnold, J. E., 1966: Easterly wave activity over Africa and in the Atlantic with a note on the intertropical convergence zone during early July, 1961. SMRP Res. Pap. No. 65, Dept. Geophys. Sci., The University of Chicago, 23 pp.

Burpee, R. W., 1971: The origin and structure of easterly waves in the lower troposphere of North Africa, Ph.D. thesis, Massachusetts Institute of Technology, 100 pp.

——, 1972: The origin and structure of easterly waves in the lower troposphere in North Africa, *J. Atmos. Sci.*, **29**, 77–90.

——, 1974: Characteristics of North African easterly waves during the summers of 1968 and 1969. *J. Atmos. Sci.*, **31**, 1556–1570.

——, 1975: Some features of synoptic-scale waves based on compositing analysis of GATE data. *Mon. Wea. Rev.*, **103**, 921–925.

——, and G. Dugdale, 1975: A summary of weather systems affecting western Africa and the eastern Atlantic during GATE. GATE Rep. No. 16, Report on the Field Phase of the GARP Atlantic Tropical Experiment Scientific Programme, Chap. 2.

Carlson, T. N., 1969a: Synoptic histories of three African disturbances that developed into Atlantic hurricanes. *Mon. Wea. Rev.*, **97**, 256–276.

——, 1969b: Some remarks on African disturbances and their progress over the tropical Atlantic. *Mon. Wea. Rev.*, **97**, 716–726.

Chang, C.-P., and C. R. Miller III, 1977: Spectrum analysis of easterly waves in the tropical Pacific during two contrasting periods of sea-surface temperature anomalies. *J. Atmos. Sci.* (in press).

Charney, J. G., and M. E. Stern, 1962: On the stability of internal baroclinic jets in a rotating atmosphere. *J. Atmos. Sci.*, **19**, 159–172.

Erickson, C. O., 1963: An incipient hurricane near the West African coast. *Mon. Wea. Rev.*, **91**, 61–68.

Frank, N. L., 1970: Atlantic tropical systems of 1969. *Mon. Wea. Rev.*, **98**, 307–314.

Hubert, H., 1939: Origine africaine d'un cyclone tropical Atlantique. *Ann. Phys. Globe France d'Outre-Mer*, **6**, 97–115.

Kuo, H. L., 1949: Dynamic instability of two-dimensional nondivergent flow in a barotropic atmosphere. *J. Meteor.*, **6**, 105–122.

Marks, F., 1975: Study of diurnal variations in convection using Quadra radar, phase I and II. GATE Rep. No. 14, Preliminary Scientific Results of the GARP Atlantic Tropical Experiment, Vol. I, 191–204.

Manabe, S., J. L. Holloway, Jr., and H. M. Stone, 1970: Tropical circulation in a time-integration of a global model of the atmosphere. *J. Atmos. Sci.*, **27**, 580–613.

Martin, D. W., 1975: Characteristics of west African and Atlantic cloud clusters based on satellite data. GATE Rep. No. 14, Preliminary Scientific Results of the GARP Atlantic Tropical Experiment, Vol. I, 182–190.

Nitta, T., 1970: A study of generation and conversion of eddy available potential energy in the tropics. *J. Meteor. Soc. Japan*, **48**, 524–528.

Norquist, D. C., E. E. Recker and R. J. Reed, 1977: The energetics of African wave disturbances as observed during phase III of GATE. *Mon. Wea. Rev.*, **105**, 334–342.

O'Brien, J. J., 1970: Alternative solutions to the classical vertical velocity problem. *J. Appl. Meteor.*, **9**, 197–203.

Pedgley, D. E., and T. N. Krishnamurti, 1976: Structure and behavior of a monsoon cyclone over West Africa. *Mon. Wea. Rev.* **104**, 149–167.

Piersig, W., 1936: Schwankungen von Luftdruck und Luftbewegung sowie ein Beitrag zum Wettergeschehen in Passatgebiet des östlichen Nordatlantischen Ozeans. *Arch. Deut. Siewarte.*, **54**, No. 6 [Parts II and III have been translated—1944: The cyclonic disturbances of the subtropical eastern North Atlantic, *Bull. Amer. Meteor. Soc.*, **25**, 2–17.]

Reed, R. J., and E. E. Recker, 1971: Structure and properties of synoptic-scale wave disturbances in the equatorial western Pacific. *J. Atmos. Sci.*, **28**, 1117–1133.

Regula, H., 1936: Druckschwankungen und Tornados an der Westküste von Afrika. *Am. Hydrogr. Mar. Meteor.*, **64**, 107–111.

Rennick, M. A., 1976: The generation of African waves. *J. Atmos. Sci.*, **33**, 1955–1969.

Riehl, H., 1954: *Tropical Meteorology*, McGraw-Hill, 392 pp.

Schubert, W. H., and R. J. Reed, 1975: Vertical motion and vorticity in the A/B scale area: phase II. GATE Rep. No. 14, Preliminary Scientific Results of the GARP Atlantic Tropical Experiment, Vol. I, 137–144.

Seguin, W., P. Gross and P. Sabol, 1976: Statistics of surface meteorological variables for the GATE A/B, B and C arrays. Paper presented at 10th Conference on Hurricanes and Tropical Meteorology, Charlottesville, Va., Amer. Meteor. Soc.

Simpson, R. H., and J. Simpson, 1975: Implications from the GATE drop windsonde program regarding A-scale circulations. GATE Rep. No. 14, Preliminary Scientific Results of the GARP Atlantic Tropical Experiment, Vol. I, 1–11.

——, N. Frank, D. Shideler and H. M. Johnson, 1968: The Atlantic hurricane season of 1967. *Mon. Wea. Rev.*, **96**, 251–259.

——, ——, —— and ——, 1969: The Atlantic hurricane season of 1968. *Mon. Wea. Rev.*, **97**, 240–255.

Wallace, J. M., 1971: Spectral studies of tropospheric wave disturbances in the tropical western Pacific. *Rev. Geophys. Space Phys.*, **9**, 557–612.